8-9-2015

Infrared surface phonon polariton waveguides on SiC Substrate

Yuchen Yang

Franklin Muriuki Manene

Brian A. Lail

Infrared Surface Phonon Polariton Waveguides on SiC Substrate

Yuchen Yang, Franklin M. Manene and Brian A. Lail
Electrical & Computer Engineering, Florida Institute of Technology, Melbourne, FL, USA 32901

ABSTRACT

Surface plasmon polariton (SPP) waveguides harbor many potential applications at visible and near-infrared (NIR) wavelengths. However, dispersive properties of the metal in the waveguide yields weakly coupled and lossy plasmonic modes in the mid and long wave infrared range. This is one of the major reasons for the rise in popularity of surface phonon polariton (SPhP) waveguides in recent research and micro-fabrication pursuit. Silicon carbide (SiC) is a good candidate in SPhP waveguides since it has negative dielectric permittivity in the long-wave infrared (LWIR) spectral region, indicative that coupling to surface phonon polaritons is realizable. Introducing surface phonon polaritons for waveguiding provides good modal confinement and enhanced propagation length. A hybrid waveguide structure at long-wave infrared (LWIR) is demonstrated in which an eigenmode solver approach in Ansys HFSS was applied. The effect of a three layer configuration i.e., silicon wire on a benzocyclobutene (BCB) dielectric slab on SiC, and the effects of varying their dimensions on the modal field distribution and on the propagation length, is presented.

Keywords: Infrared waveguide, surface phonon polariton, hybrid waveguide, silicon carbide, LWIR.

1. INTRODUCTION

The temporal resolution of detector and the study of spectroscopy motivates research into infrared (IR) and optical structures capable of guiding light with sub wavelength confinement[1,19]. There are numerous studies in surface plasmon polariton waveguides[1,2,11,12] and they have applications such as plasmonic nanolithography[22], near-field scanning optical spectroscopy (SNOM)[23], data storage[18], and biosensing[24]. The SPPs are transverse surface charge waves accompanying electromagnetic fields localized at an interface between a metal and a dielectric at the visible and near-IR region[5,13]. However, plasmonic applications in the IR/THz are limited by the low confinement of coupled modes along conductor/dielectric boundaries due to the large permittivity magnitude of metals in this region of the spectrum as well as high metal losses. Several studies have considered traditional microstrip and two-wire transmission line structures, however, unacceptably short propagation lengths resulted[9, 10].

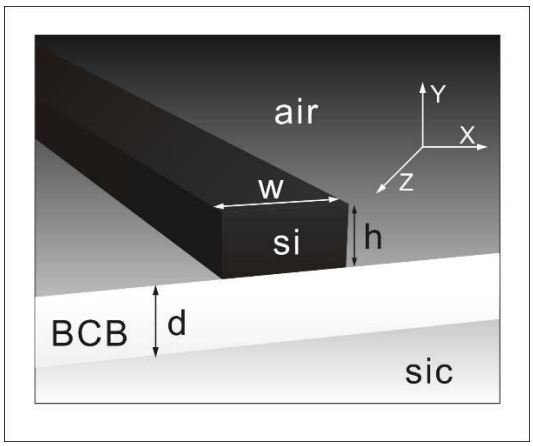

Figure 1. Hybrid SPhP waveguide geometry.

A new approach is eliminate the disadvantage of SPPs by using Surface Phonon Plaritons (SPhPs) -a collective excitation comprised of an electromagnetic (EM) wave coupled with polar lattice vibration[16], whose electromagnetic field decays exponentially away from the interface and thus provides strong confinement[14,25]. This hybrid waveguide consists of a rectangular, dielectric silicon wire separated from silicon carbide by a dielectric spacer of lower electrical permittivity than

Plasmonics: Metallic Nanostructures and Their Optical Properties XIII, edited by Allan D. Boardman, Din Ping Tsai,
Proc. of SPIE Vol. 9547, 954723 · © 2015 SPIE · CCC code: 0277-786X/15/$18 · doi: 10.1117/12.2188605

that of the wire. The schematic diagram of the hybrid phonon polariton LWIR waveguide is shown in Fig. 1. Integrated polaritonics has the potential to revolutionize next-generation devices operating in the THz portion of the electromagnetic spectrum in much the same way that integrated electronics and integrated photonics have revolutionized the microwave and near-infrared regimes, respectively. In this study, silicon carbide (SiC) has been used because, at mid-infrared frequencies it has desirable material properties. Since its optical response is similar to metals[6], it is an alternative to metals; its real permittivity is negative and a sharp resonance near 24THz (12.5μm) manifests itself by way of excitation of transverse optical phonons[17].

2. SIMULATION METHOD AND MODAL PROPERTIES OF THE HYBRID SURFACE PHONON POLARITON WAVEGUIDES

Fundamentally, SPhP waves are transverse magnetic surface waves propagating along the interface between two materials of negative and positive dielectric function. The surface phonon polarition existence condition $\varepsilon < -1$ is satisfied for between the longitudinal (LO) and transverse (LO) optical phonon resonances crystalline silicon carbide (c-SiC) in the mid-IR spectral range between 10.3 μm and 12.6 μm as is shown in Fig. 2 and it is an attractive wide bandgap semiconductor for high-temperature and high-power microelectronics[26]. As a polar dielectric, SiC supports strong SPhP resonances in the infrared region around 11μm [8]. Also research shows that infrared dipole antennas formed on a SiC substrate can achieve a field enhancement on the order of 10^7 [4,15]. Compared to flexible and lossy metals, SiC has a considerably higher Young's modulus and lower optical damping constant. The longer wavelength SPhP in SiC can also induce stronger coupling and larger optical forces for similarly sized structures [8].The dispersion relation for the wave vector of the SPhPs is given by [20]:

$$\mathrm{k_{SPhP}}(\omega) = \frac{\omega}{\mathrm{c}}\sqrt{\frac{\epsilon_1(\omega)\epsilon_2}{\epsilon_1(\omega)+\epsilon_2}} \tag{1}$$

From eq. 1, the real and imaginary components for the dispersion relationship are:

$$\mathrm{k_{SPhP}}(\omega) = \frac{\omega}{\mathrm{c}}\left(\frac{\epsilon_1'(\omega)\epsilon_2}{\epsilon_1'(\omega)+\epsilon_2}\right)^{1/2} + \mathrm{j}\frac{\omega}{\mathrm{c}}\left(\frac{\epsilon_1'(\omega)\epsilon_2}{\epsilon_1'(\omega)+\epsilon_2}\right)^{2/3}\frac{\epsilon_1''(\omega)}{2(\epsilon_1')^2} \tag{2}$$

Where k_{SPhP} is the wave vector of the SPhPs, $\varepsilon_1'(\omega)$and, $\varepsilon_1''(\omega)$ are the real and imaginary parts of the dielectric constants for SiC respectively, and ε_2 is the permittivity of the benzocyclobutene (BCB) spacer. Fig. 3 shows the dispersion relation of the SPhP waveguide at the BCB-SiC interface. The resonant condition between the two media is $Re[\varepsilon_1(\omega)] = -\varepsilon_2$, so from the Fig. 3 it has a phonon resonance at 10.8μm with negative dielectric permittivity in the LWIR spectral range between 10.3 and 12.6μm.

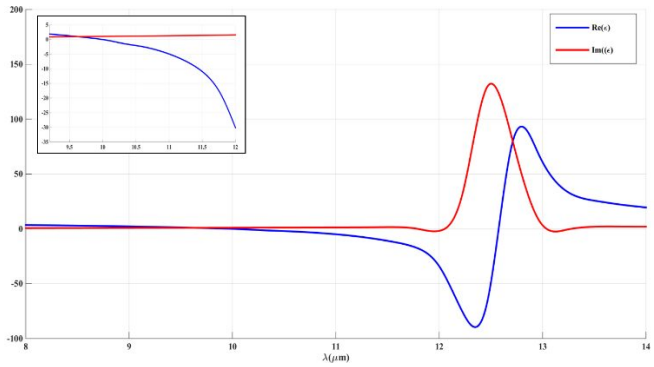

Figure 2. Real and imaginary parts of the dielectric permittivity of SiC.

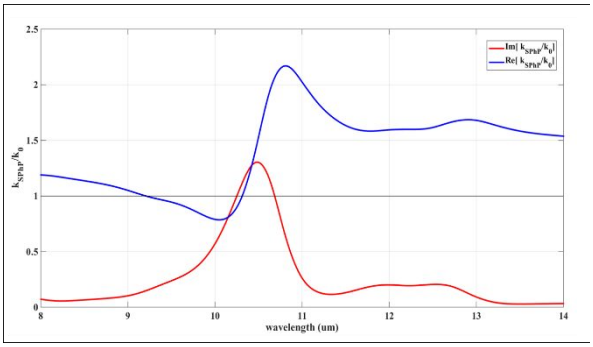

Figure 3. Real and imaginary parts of the dispersion relation for SPhPs at BCB-SiC interface are calculated according to Eq.(1).

The propagation distance given by[27]:

$$L = [2Im\{k\}]^{-1} \tag{3}$$

Where k is the wave number of the mode of interest.
In addition to this, the attenuation constant, $\alpha = Im\{k\}$ is expressed as[27]:

$$\alpha = P_{loss}/P_{trans} \tag{4}$$

Where P_{loss} is the total power loss in the waveguide and P_{trans} is the transmitted power; these values can be calculated by using eigenmode field calculator in HFSS (Ansoft). The modal area (A_m) is defined as the ratio of the total modal energy per unit length to the peak energy density along the propagation direction [7].

$$A = \frac{W_m}{max\{W(r)\}} = \frac{1}{max\{W(r)\}} \iint W(r) d^2r \tag{5}$$

where *W(r)* is the energy density given by

$$Wr = \frac{1}{2}\left(\frac{d(\epsilon(r)\omega)}{d\omega}|E(r)|^2 + \mu_0|H(r)^2|\right) \tag{6}$$

Here E(r) and H(r) are the electric and magnetic fields,$\epsilon(\omega)$ is the electric permittivity, μ_o is the magnetic permeability. Mode confinement can be gauged by the normalized mode area which is defined as A_m/A_o where $A_o = \lambda_o^2/4$ and λ_o is the free space wavelength. This compares the mode volume to the standard diffraction limit, as in dielectric waveguide.

3. RESULTS OF NUMERICAL SIMULATIONS

We apply an eigensolver approach simulation in Ansys HFSS, the accuracy and versatility of the method used has been tested in [3], where results in [21] based on semi-analytical methods of lines had been reproduced. We can achieve efficient complex eigen frequencies by changing the phase delay between the boundaries parallel to the propagation direction, whereas the remaining boundaries are combinations of perfect electric and magnetic walls placed far enough from the wire to leave the hybrid modes unperturbed.

By tuning the geometry of the structure, we can achieve reasonable propagation length and maintain moderate field confinement. As shown in Fig.2 the three-layered hybrid waveguide constructed by the high permittivity rectangular Si wire $\varepsilon_{Si} = 11.7\mu m$ (rectangular waveguide) attached on a low permittivity dielectric BCB spacer with permittivity $\varepsilon_{BCB} = 2.34\mu m$ on top of a SiC wafer with permittivity $\varepsilon_{SiC} = -30.55 + i1.57$ (phonon waveguide) . We have analyzed the influence of the width of the silicon wire (*w*) on the propagation characteristics of the hybrid SPhP waveguide. If *w* is set below 2.25μm, we can get lower propagation loss, however, the field would be weakly confined. In contrast, if *w* is larger

than 2.25μm, the mode will be more Si-wire like. In the following result, w is fixed at 2.25μm and the rectangular wire height h and the spacer height between the wire and the SiC wafer d are varied. The propagation length L(μm), mode area A_m and electromagnetic field distribution at wavelength, $\lambda = 12.002\mu m$ are presented.

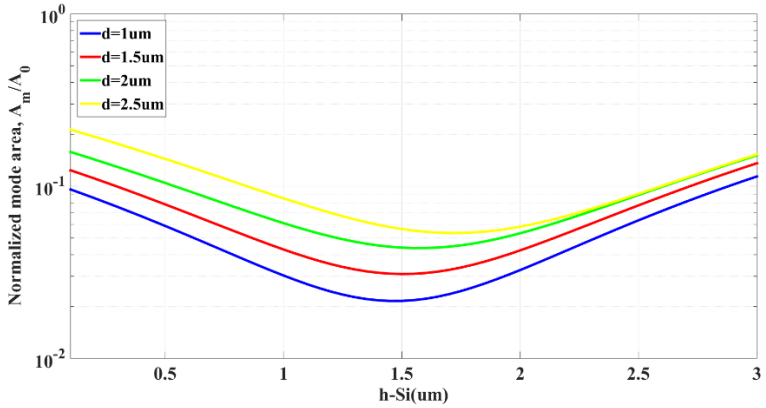

Figure 4. Modal area, A_m/A_0versus the Si thickness h for different thickness of the BCB layer d.

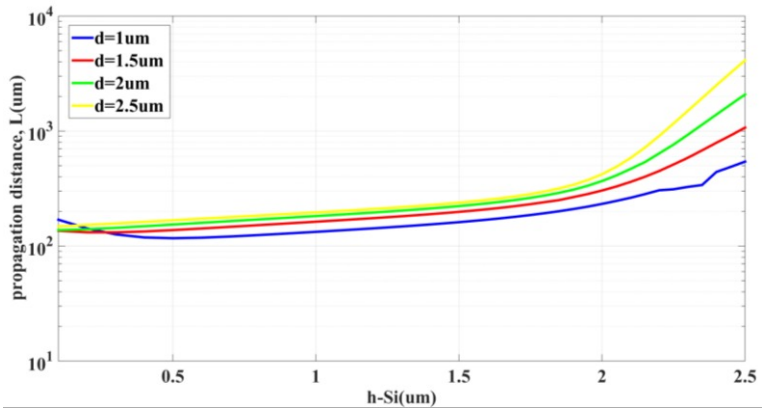

Figure 5. The hybrid mode's propagation distance versus the Si thickness h for different thickness of the BCB layer d.

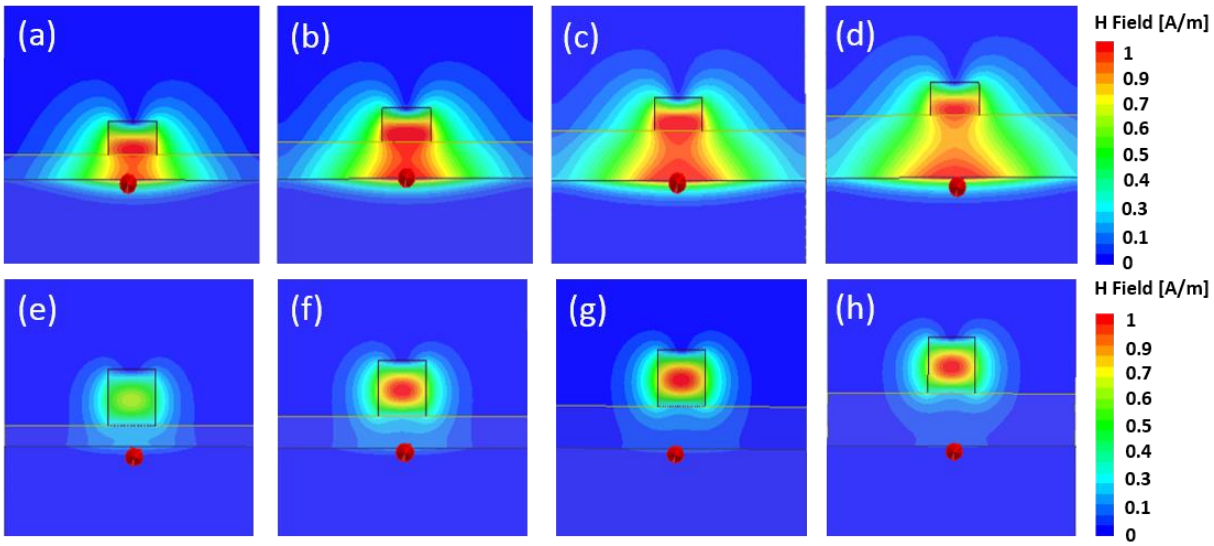

Figure 6. (a) Complex magnitude of H for [h,d]=[1.35,1]μm. (b) [h,d]=[1.35,1.5]μm. (c) [h,d]=[1.35,2]μm. (d)[h,d]=[1.35,2.5]μm. (e) [h,d]=[2.65,1]μm. (f) [h,d]=[2.65,1.5]μm. (g) [h,d]=[2.65,2]μm. (h) [h,d]=[2.65,2.5]μm.

Figure 4 and 5 shows the dependence of normalized modal area and propagation distance. For large h, the hybrid waveguides that tend to support low-loss rectangular dielectric waveguide modes with electromagnetic filed are mainly confined in the high-permittivity Si wire [Fig.6 (e)-(h)]. In this case, the propagation length is much bigger than other modes, but at the cost of much larger mode area (low confinement). At moderate dimensions of h and d, mode coupling results in a new hybrid mode that shows both Si wire and SiC phonon modes; the magnetic intensity field is distributed over both the Si rectangular waveguide and the SiC-BCB interface [Fig. 6 (a)-(d)]. By keeping the height of Si to be 1.35μm and increasing the height of the BCB spacer *d*, we can achieve increase in propagation length from 151.06μm to 222.67μm while still keeping the hybrid mode confined [Fig. 6 (a)-(d)]. We have seen that from the normalized mode area, the lowest mode area is near $h = 1.5\mu m$, for all variations of d. Besides, lower refractive index of the inner BCB dielectric layer will ensure relatively lower propagation loss because the field inside the SiC would much weaker.

4. COMPARISON WITH THE HYBRID WAVEGUIDE AT DIFFERENT WAVELENGTH

From the previous section, it has been shown that the hybrid SPhP waveguide was able to guide the SPhP modes with favorable mode area and propagation distance due to the involvement of low loss dielectric BCB and interaction with negative permittivity SiC coupling with high index Si. We are also interested in the hybrid mode characteristics including mode confinement and propagation distance at other wavelengths. The comparison of the field distribution demonstrates at 11.174μm, 11.78μm and 12.002μm and is shown in Fig.7 for dielectric BCB spacer equal to $0.25\mu m$ and $2\mu m$.

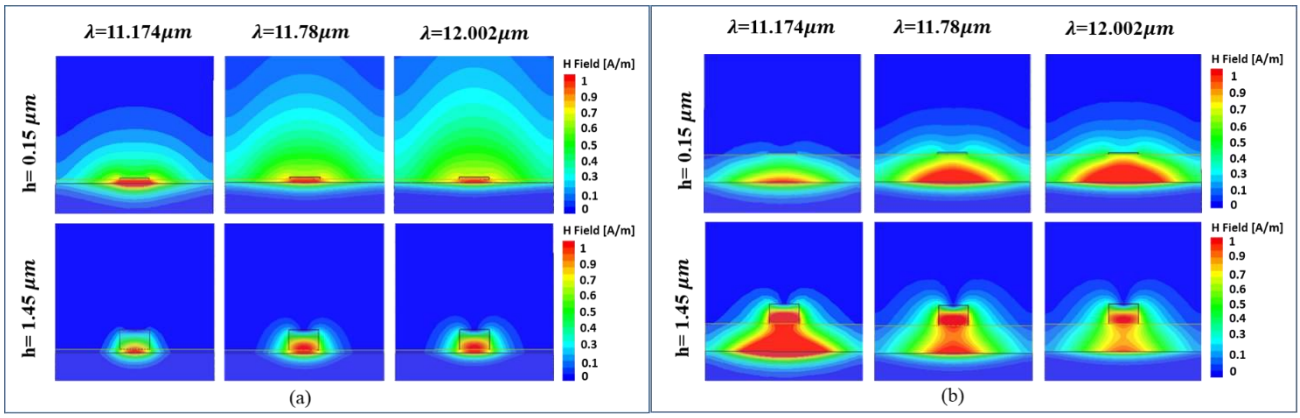

Figure 7. H-Field distribution for $d = 0.25\mu m$ (a) and $d = 2\mu m$ (b).

We have seen that the field distribution is not confined for short Si height but the strongest field is in the BCB spacer in Fig.7 (a) top row, by increasing the wavelength there are more fields that are unbounded from the structure. But by increasing the height of Si and keeping other dimensions the same, the field is concentrated close to the spacer. We find that the propagation length in the waveguide at 12.002μm is 416.65μm, which is longer when compared to 11.61μm at $\lambda = 11.174\mu m$. Fig.7 (a) bottom row, there is a decrease of the propagation length with increase in frequency, which can be predicted mathematically and consequently numerically by equation 3. From Fig.7 (b) top row, it is seen that that the phonon mode strength increases by increasing the wavelength. At appropriate dimensions the hybrid mode exists, however more hybrid modes can be formed at $\lambda = 11.174\mu m$ but the propagation distance is much less than the hybrid modes at $\lambda = 12.002\mu m$. Mode area seems to be keeping in with the same trend. This means that the hybrid waveguide has good performance at lower frequencies. An interesting observation is that, propagation lengths deteriorates at wavelengths closer to the phonon resonance of SiC.

5. CONCLUSION

We have proposed a hybrid surface phonon polariton waveguide by coupling Si and SiC based phonon modes through finite element analysis using an eigenmode solver. By controlling the hybridization of the fundamental mode of a rectangular dielectric wire (Si) and the phonon mode of a dielectric-negative permittivity material (SiC), we achieve field confinement and long-range propagation. We observed that for free-space wavelength $\lambda = 12.002\mu m$, propagation length $L = 18.55\lambda = 222.6\mu m$, while maintaining well-confined modes. Also by comparing the modal area and propagation length for different wavelengths-$\lambda = 11.174\mu m$, $\lambda = 11.78\mu m$, $\lambda = 12.002\mu m$, the best performance of field distribution and propagation distance appears to be for $\lambda = 12.002\mu m$.

REFERENCES

[1] R. F. Oulton, V.J. Sorger, D.A. Genov, D.F. P. Pile, and X. Zhang, "A hybrid plasmonic waveguide for subwavelength confinement and long- range propagation," Nature Photonics 2, 496-500 (2008).

[2] L. Chen, X. Li, G. Wang, W. Li, S. Chen, L. Xiao, and D. Gao, "A silicon based 3-D hybrid long-range plasmonic waveguide for nanophotonic integration," Journal Lightwave Technology 30, 163-168 (2012).

[3] A. Degiron, and D. R. Smith, "Numerical simulations of long range plasmons," Optics Express 14(4), 1611-1625 (2006).

[4] H. Kim and X. Cheng, "Infrared dipole antenna enhanced by surface phonon polaritons," Optics Letters 35 (22), 3748-3750 (2010).

[5] I. Avrutsky, R. Soref, and W. Buchwald, "Sub-wavelength plasmonic modes in a conductor–gap- dielectric system with a nanoscale gap," Optics Express 18(1), 348-363 (2010).

[6] J. A. Schuller, R. Zia, T. Taubner, and M.L. Brongersma, "Dielectric metamaterials based on electric and magnetic resonances of silicon carbide particles," Physical Review Letter 99, 107401 (2007).

[7] Huber A.J, Deutsch.B, Novotny L, and Hillenbrand R. "Focusing of surface phonon polaritons," Applied Physics Letters 92, 203104-1 (2008).

[8] D. Li, N. M. Lawandy, and R. Zia, "Surface phonon-polariton enhanced optical forces in silicon carbide nanostructures," Optics Express 21(18), 20900-20910 (2013).

[9] T. Mandviwala, B. Lail, and G. Boreman, "Infrared-frequency coplanar striplines: design, fabrication, and measurements," Microwave and Optical Technology Letters 47(1), 17-20 (2005).

[10] T. Mandviwala, B. Lail, and G. Boreman, "Characterization of microstrip transmission lines at IR frequencies-modeling, fabrication and measurements," Microwave and Optical Technology Letters 50 (5), 1232-1237 (2008).

[11] L. Chen, T. Zhang, X. Li, and W. Huang, "Novel hybride plasmonic waveguide consisting of two identical dielectric nanowires symmetrically placed on each side of a thin metal film," Optics Express 20(18), 20535-20544 (2012).

[12] M. Z. Alam, J. Meier, J. S. Aitchison, and M. Mojahedi, "Propagation characteristics of hybrid modes supported by metal-low-high index waveguides and bends," Optics Express 18(12), 12971-12979 (2010).

[13] H. Raether, [Surface Plasmons], Springer-Verlag, Berlin, (1988).

[14] S. A. Holmstrom, J. B. Khurgin, and R. Ghodssi, "Guided-mode phonon-polaritons in suspended waveguides," Physical Review B 86(16), 165120 (2012).

[15] A. Huber, N. Ocelic, D. Kazantsev, and R. Hillenbrand "Near-field imaging of mid-infrared surface phonon polariton propagation," Applied Physical Letters 87 (2005).

[16] D.Z.A. Chen and G. Chen, "Measurement of silicon dioxide surface phonon-polariton propagation length by attenuated total reflection," Applied Physical Letters 91(12), 121906-1 - 12906-3 (2007).

[17] V. M. Shalaev, "Optical negative-index metamaterials," Nature Photonics 1, 41-48 (2007).

[18] N. Ocelic and R. Hillenbrand, "Subwavelength-scale tailoring of surface phonon polaritons by focused ion-beam implantation," Nature materials 3, 606-609 (2004).

[19] M. Z. Alam, J. Meier, J. S. Aitchison, and M. Mojahedi, "Super mode propagation in low index medium," Conference on Lasers and Electro-Optics, (2007).

[20] F. Manene, E. C. Kinzel and B. Lail, "Finite element eigenmode analysis of hybrid surface phonon polariton infrared waveguides," Applied Computational Electromagnetics, 297-302, (2014).

[21] P. Berini, "Plasmon-polariton waves guided by thin lossy metal films of finite width: bound modes of symmetric structures," Physical Review B 61, no. 12, 125417 (2000).

[22] W. Srituravanich, N. Fang, C. Sun, Q. Luo, and X. Zhang, "Plasmonic Nanolithography," Nano Letters 4(6),1085-1088 (2004).
[23] T. Klar, M. Perner, S. Grosse, G. von Plessen, W. Spirkl, and J. Feldmann, "Surface-Plasmon resonances in single metallic nanoparticles," Physical Revew Letters 80, 19 (1998).
[24] J. N. Anker, W. P. Hall, O. Lyandres, N. C. Shah, J. Zhao and R. P. Van Duyne, "Biosensing with plasmonic nanosensors," Nature materials 7, 442-453 (2008).
[25] V. M. Agranovich and D. L. Mills, [Surface Polaritons Electromagnetic Waves at Structures and Interfaces], North-Holland (1982).
[26] A. Kumar and M. S. Aspalli, "SiC: An advanced semiconductor material for power devices," International Journal of Research In Engineering and Technology 3, 248-252 (2014).
[27] F. Manene, B. Lail, and E. C. Kinzel, "Waveguiding of surface phonon polariton," IEEE AP-S Conference, (2013).